Carbon Trends 5 (2021) 100090

Contents lists available at ScienceDirect

Carbon Trends

journal homepage: www.elsevier.com/locate/cartre

A mechanism study of acid-assisted oxidative stabilization of asphaltene-derived carbon fibers

Desirée Leistenschneider, Peiyuan Zuo, Yuna Kim, Zahra Abedi, Douglas G. Ivey, Arno de Klerk, Xuehua Zhang, Weixing Chen*

Department of Chemical and Materials Engineering, University of Alberta, Edmonton, Alberta, Canada T6G 2V4

ARTICLE INFO

Article history:
Received 5 April 2021
Revised 16 July 2021
Accepted 1 August 2021

Keywords:
Asphaltene
Carbon fiber
Low softening point
Melt spinning
Oxidative stabilization

ABSTRACT

The development of inexpensive carbon fiber precursors is necessary to meet the future demands of carbon fibers. This work shows how asphaltenes, which are obtained as a by-product in bitumen production, can play an important role as such inexpensive carbon fiber precursors. To synthesize carbon fibers from asphaltene, stabilization by means of oxidizing acids (HNO_3 and H_2SO_4) was developed. Stabilization could not be achieved by a non-oxidizing acid (HCl). The reactions leading to fiber stabilization was investigated for nitric acid treatment, which led to oxidation and the incorporation of nitro-groups. Further thermal treatment caused an increase in C/H ratio that was related to decomposition of nitro-groups, which facilitated air oxidation and other reactions leading to the loss of volatile hydrogen-rich products, such as light hydrocarbons. Additionally, the influence of the acid concentration during treatment on fiber properties, such as fiber diameter, composition, tensile strength and elastic modulus, has been examined. The application of the acid treatment leads to carbon fibers with good tensile properties, with a tensile strength and elastic modulus of 811 MPa and 32.7 GPa, respectively. The overall yield of carbon fibers is 37 – 38 wt.%.

1. Introduction

Carbon fibers are characterized by their high specific strength, high electronic conductivity, mechanical stability and thermal insulating property. As a consequence, they are applied in several applications such as structural materials [1], energy storage devices [2] and thermal insulation [3]. The demand for carbon fibers has been increasing by ~12% every year over the past 20 years, especially in the development of light weight automotive components [4]. Typical precursors for carbon fibers are coal, petroleum or plant-based pitches, as well as polyacrylonitrile (PAN). The latter shows excellent mechanical properties with high tensile strengths of 3 to 7 GPa and tensile elastic moduli of 200 to 350 GPa [4,5]. However, the low carbon fiber yield and the expensive monomers for PAN represent a major drawback for a widespread application [6]. The use of pitches, especially isotropic pitches; however, results in lower production costs at the expense of tensile strength and elastic modulus [7]. Because almost 50% of the total carbon fiber cost originates from the fiber precursor, one of the key fabrication steps is to use inexpensive precursors and to develop methods to improve the mechanical properties of such fibers [8,9].

Carbon fiber production includes several process steps. Precursors are initially extruded into fibers *via* spinning of the precursor. The resulting fibers from this step are called 'green fibers'. Melt spinning is the preferred procedure for precursors that soften below 400°C, due to its low production costs and the absence of solvents [10,11]. To transform the green fibers into carbon fibers, the green fibers are processed at high temperatures up to 2000°C in nitrogen, through 'carbonization'. However, the green fibers are prone to melting during this high temperature step. To prevent melting of the material and, therefore, the loss of the fiber structure, the green fibers are usually oxidized in air during a so-called 'oxidative stabilization' step prior to carbonization.

During oxidative stabilization, also known as the stabilization step, the green fibers are oxidized in air, typically at temperatures 30–50°C below the softening point of the precursor and up to 300°C. During this step, oxidative cross-linking reactions between heteroatom-containing groups are initiated which stabilize the fiber structure [12–15]. These findings are based on isotropic pitch-based, PAN-based and mesophase pitch-based carbon fibers. Depending on the starting material, and its composition and soft-

* Corresponding author.
E-mail address: weixing@ualberta.ca (W. Chen).

https://doi.org/10.1016/j.cartre.2021.100090

ening point, a suitable stabilization process has to be found. Since the oxidative process step is the most time and cost intensive, efforts have been made to shorten the oxidation step. For example, Yonemoto *et al.* found that the addition of NO_2 to the air atmosphere increases the oxidation degree of the fibers [16]. Based on these findings, Vilaplana-Ortego *et al.* showed that the treatment of petroleum pitch-based green fibers with dilute HNO_3 can significantly reduce the oxidation time from 60 h to only 6 h [17]. Especially for promising inexpensive precursors, which exhibit a low softening point, finding a suitable oxidation process can be critical to the development of cost effective high-performance carbon fibers.

One material which is a promising carbon fiber precursor, with a low softening point, is asphaltenes. Asphaltenes is a solubility class of petroleum, which can be separated from heavy petroleum by a solvent deasphalting process to produce a lower viscosity deasphalted oil product and an asphaltenes product [18]. In solvent deasphalting the petroleum is mixed with a light n-alkane (paraffin) causing some of the material to remain in the n-alkane rich liquid phase and some of the material, the asphaltenes, to form a separate phase. Based on current understanding, drawing from characterization by many analytical techniques, the asphaltenes has a broad molecular mass distribution with an average molecular mass of 700–750 g/mol and appear to consist mainly of polycyclic aromatic structures [19]. The high polycyclic aromatic content of the asphaltenes makes it a potentially good precursor material for carbon fiber production. Asphaltenes are mainly responsible for the high viscosity of bitumen, which complicates bitumen transport *via* pipelines and further processing [20]. Therefore, asphaltenes are removed prior to the bitumen transport and have no further value for bitumen processing. Turning those asphaltenes into carbon fiber would convert a low price by-product into a high-end product with an ever increasing demand. Since asphaltenes have a low softening point (<200°C), the successful stabilization of asphaltene-based green fibers is crucial to avoid melting of the fibers during carbonization.

This work investigates the underlying oxidative stabilization mechanism using various acids, such as HNO_3, H_2SO_4 and HCl, and salt solutions. The oxidative stabilization process of asphaltene-based carbon fibers using an acid treatment has not been investigated in detail yet. The work explores whether previous literature findings from reference [12–15], which are based on isotropic pitch-based carbon fibers are valid for asphaltene-based fibers as well. Furthermore, through acid-assisted stabilization, the industrially separated asphaltenes used in this study are shown to be suitable precursors for carbon fibers even though they exhibit a very low softening point below 200 °C. Additionally, the influence of acid concentration and the final carbon fiber diameter on the tensile properties were examined.

2. Experimental

2.1. Materials and methods

Raw asphaltene was obtained from CNOOC Ltd. (formerly Nexen Energy) from an industrial C_5 solvent de-asphalting process at the Long Lake Upgrader, AB, Canada, in 2014. The material was used without further purification. Concentrated HNO_3 (15.8 M, certified ACS plus), H_2SO_4 (17.8 M, certified ACS Plus), and HCl (6 M) were purchased from Thermo Fisher Scientific. Acids were diluted with deionized water (Milli-Q). KNO_3 was purchased as a powder (ACS reagent, ≥99.0%) was purchased from Sigma Aldrich.

Elemental composition was determined using a CHNS-O Flash2000 from Thermo Fisher Scientific with a 2,2′-(2,5-Thienediyl)bis[5-(2-methyl-2-propanyl)-1,3-benzoxazole (BBOT) standard. Samples were finely ground prior to the measurement and weight into tin crucibles. Fourier-transform infrared spectroscopy (FT-IR) spectra were recorded using a FT-IR spectrometer iS50 from Nicolet with an attenuated total reflection (ATR) module. Prior to the measurement the samples were finely ground in an agate mortar. Powder X-ray diffractograms were measured with a Ultima IV system from Rigaku. The X-ray source was CoKα, and samples were scanned from 5–90° 2θ with a scan speed of 2–2θ min^{-1} and a step size of 0.02° 2θ. Field emission scanning electron microscopy (ZEISS Sigma 300 VP-FESEM, SEM) was used for imaging fiber samples. All samples, except the carbon fibers, were coated with carbon to improve sample conductivity. Thermogravimetric analysis was conducted with a Mettler Toledo TGA/DSC1 (TGA) system equipped with an LF 1100 furnace, sample robot and MX5 internal microbalance.

To investigate the tensile properties of the single fibers, 20 specimens per batch were prepared. The specimens (gauge length = 1.27 cm) were measured with an Instron 5565 tension tester (speed: 5.72 mm min^{-1}).

2.2. Fiber fabrication

Green fibers were produced in a melt spinning process using an AT225 melt spinner purchased from Anytester, China. The raw asphaltene was melted at a temperature of 197°C and processed into asphaltene filaments by pressing the melted material through a spinneret hole with a diameter of 0.15 mm under a nitrogen pressure of 400 kPa. The green fibers were collected on a drum with a winding speed of 200 rpm and were immediately cooled to room temperature after passing through the spinneret hole. Afterwards, the fibers were dipped into diluted HNO_3 with concentrations ranging from 10 vol.% to 40 vol.% HNO_3. To investigate the type of reactions involved in stabilization, H_2SO_4, HCl and KNO_3 solutions with a concentration of 3.16 M, which corresponds to the molar concentration of a 20 vol.% HNO_3 solution were used as well. The fibers were kept in solution for 10 min without stirring. Then, without applying any washing or drying step, the fibers were heated from room temperature to 300°C in a tube furnace equipped with a quartz tube with a heating rate of 0.5°C min^{-1} under synthetic air atmosphere (flow: 400 ml min^{-1}). When only heating to 300°C under air is performed without prior acid-treatment, it is called 'one-step stabilization'. The fiber sample was naturally cooled after this oxidation process. Hence, oxidized fiber samples are designated as follows: OF_{Acid}-X, where OF stands for oxidized fiber, acid describes the acid used (HNO_3, H_2SO_4, HCl, or none) and X denotes the final temperature the fibers are subjected to for stabilization, i.e. room temperature (RT), 140°C or 230°C in Section 3.3, whereas in Section 3.4 is describes the acid concentration used prior to the oxidative stabilization step. Oxidized fibers that are subjected to the complete one-step stabilization process until a temperature of 300°C will be denoted as OF_{Acid} to circumvent a too long sample name. As the last step, the oxidative stabilized fibers were carbonized at 1500°C for 2 h with a heating rate of 3°C min^{-1} starting from room temperature under N_2 (purity 5.0, flow: 400 ml min^{-1}) in a tube furnace equipped with an alumina tube. Carbon fibers are designated as CF-X, where CF stands for carbon fiber and X describes the acid concentration, which was used prior to the oxidative stabilization.

3. Results and discussion

3.1. Acid treatment

As mentioned above, the prevention of the fiber melting during carbonization at high temperature is necessary. A comparison of the one-step stabilization process, which took 9 h to complete, was

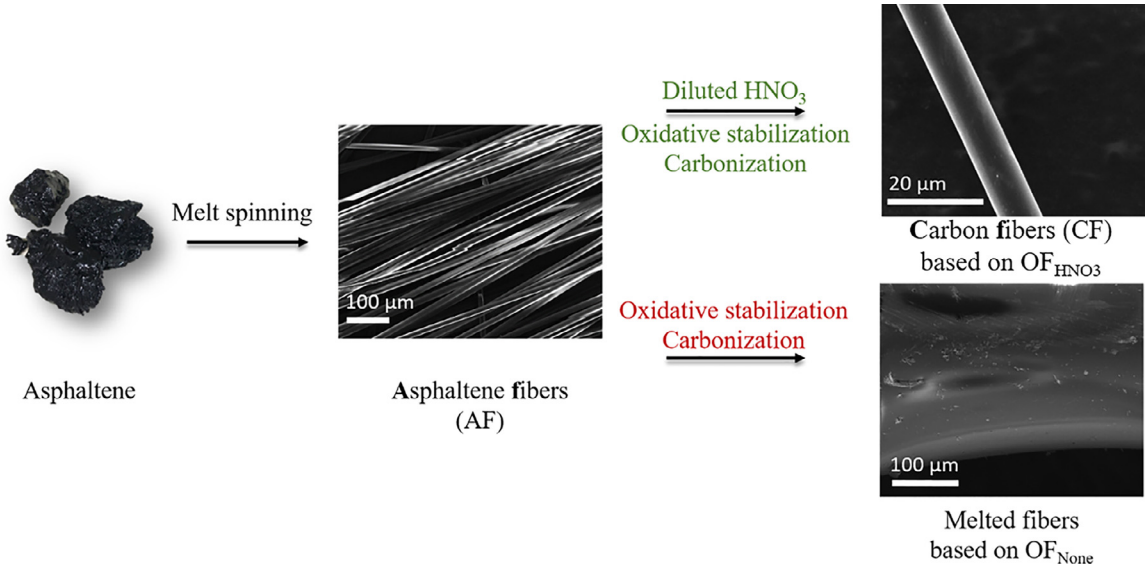

Fig. 1. Process overview including SEM secondary electron (SE) micrographs of asphaltene fibers (AF), acid treated oxidized fibers (OF_{HNO3}) and oxidized fibers without pre-acid treatment (OF_{None}).

Table 1
Elemental composition of AF and different OFs determined *via* elemental analysis.

	Element content[a] / wt.%					Molar ratios			
Sample	C	H	N	S	O[b]	C/H	C/N	C/S	C/O
AF	82.25	8.10	1.05	7.72	0.88	0.85	91.4	28.5	125
OF_{None}	80.72	7.38	1.12	7.47	3.31	0.91	84.1	29.3	32.5
OF_{HNO3}	66.75	2.81	1.93	6.38	22.13	1.98	40.4	34.8	4.0
OF_{H2SO4}	69.26	3.52	1.56	7.05	18.25	1.64	51.8	32.1	5.1
OF_{HCl}	81.04	7.44	1.12	7.60	2.80	0.91	84.4	34.6	38.6
OF_{KNO3}	59.72	5.08	4.22	4.05	26.93	0.98	16.5	38.3	4.8
$OF_{HClKNO3}$	- [c]	- [c]	- [c]	- [c]	- [c]	- [c]	- [c]	- [c]	- [c]
OF_{HNO3}-RT	78.02	7.60	1.99	7.30	5.10	0.86	45.7	32.1	20.4
OF_{HNO3}-140	74.77	7.00	2.80	6.99	8.76	0.89	31.2	32.1	11.4
OF_{HNO3}-230	72.99	6.16	2.90	7.00	10.95	0.99	29.4	31.3	8.9

[a] Values are obtained as an average from 3 measurements (with a standard deviation smaller than 5%), or 2 measurements if the composition difference was smaller than 5%.
[b] O content is calculated from the residual mass. Other components in the precursor material such as V and Ni are below 1500 ppm (determined *via* XRF, Supporting information Table S1). It is assumed that these element contents are constant for all fibers and therefore, changes in residual mass content are only due to changes in O content.
[c] Not available, only analyzed by EDX.

made with nitric acid pretreatment followed by the same oxidative stabilization. It was found that when conducting the oxidative stabilization of asphaltene fibers (AF) without acid pretreatment, the fibers did not retain their fibrous shape (Fig. 1). When starting with industrially precipitated asphaltenes it was not viable to consider the one-step stabilization process.

The oxidized fibers with and without acid treatment have considerable composition differences, with a lower molar C/H ratio for OF_{None} (0.91) than for OF_{HNO3} (1.98) (Table 1). In addition, OF_{HNO3} shows a higher oxygen content. Both a higher C/H ratio and a higher oxygen content point to stronger oxidation of the acid treated sample OF_{HNO3}. Using the one-step oxidation (OF_{None}) leads to the reduction of C/N and C/O to 84.03 and 32.52, respectively. These compositional changes are not as pronounced as for OF_{HNO3}, which shows a C/N and C/O ratio of 40.35 and 4.02, respectively. The reason for this could be either a stronger reaction such as oxidation, incorporation of N and O, leading to carbon with a higher extent of oxidation, or evaporation of smaller carbon containing molecules. Details on these reactions will be discussed in a later section.

3.2. Reactions leading to fiber stabilization

This section investigates the role of HNO_3 during the oxidation process. Chemically, HNO_3 can act in four different ways: (i) as an acid, (ii) as an oxidizing agent, (iii) as a nitrating agent, and (iv) as a source of nitrate (NO_3^-). As an acid, it was anticipated that it would promote cross-linking by acid catalysis and potentially some ion exchange with cations already present in the material. As an oxidizing agent, oxidation results from decomposition reactions to release NO_x, which simultaneously could lead to oxidation of the material, or water elimination from the material [21]. As a nitrating agent, nitro-groups ($-NO_2$) can be introduced by nitric acid and several such reactions were described [22,23]. Vilaplana-Ortego *et al.* found that HNO_3 introduces NO_2-and oxygen-containing functional groups, which remain on the fibers even after the oxidative heat-treatment [17]. As a source of nitrate, it could ion exchange with anions already present in the material, be adsorbed, or retained in an emulsified form.

To study the manner in which HNO_3 prevents fusing of fibers, green fibers were subjected to three different chemical treatments

of the same molar concentration: H_2SO_4 as an oxidizing acid comparable to HNO_3, HCl as a non-oxidizing acid and KNO_3 as a neutral, oxidizing, NO_3^- providing salt.

Only HNO_3 and H_2SO_4 led to a fiber structure retention, whereas the use of KNO_3 and HCl resulted in the melting of fibers during heat treatment. Acid catalyzed conversion, if it took place, in the absence of oxidation was ineffectual. The nitrate ion in the absence of acidity also did not have an observable impact. Since both HNO_3 and H_2SO_4 led to a fiber structure retention, it was possible that HNO_3 played a dual role during the treatment process, as an acidic catalyst and as an oxidizing agent. Although nitration by HNO_3 likely took place [17], it was not a reaction that was a prerequisite for fiber structure retention.

In addition, significant differences in the elemental composition are seen in successfully stabilized fibers and melted fibers (Table 1). The fibers that maintain their structure, OF_{HNO3} and OF_{H2SO4}, have a C/H ratio of 1.98 and 1.64, respectively. On the other hand, the C/H ratio for the melted fibers, OF_{HCl} and OF_{KNO3}, remains low (0.91 and 0.97, respectively) and is comparable to the C/H ratio for the non-treated fiber, OF_{None}. Thus, a significant increase in C/H is crucial for fiber stabilization.

There is more than one reaction that can result in an increase in the C/H ratio. The two reactions that are the most likely to lead to an increase in C/H in asphaltene-based fibers are: (i) Hydrogen disproportionation leading to cross-linking and elimination of hydrogen-enriched volatile products, and (ii) the elimination of hydrogen by oxidation, with or without the introduction of oxygen-containing surface groups. The oxygen groups are able to undergo condensation reactions forming C-O-C groups which could further stabilize the fiber structure in a manner equal to the cross-linking forming C-C bonds [24]. Oxygen-containing functional groups can also participate in reactions to form C-C bonds, for example, aldol condensation. The study by Vilaplana-Ortego *et al.* shows the formation of oxygen-containing groups on the surface of isotropic pitch-based carbon fibers and the elimination of hydrogen concomitant with C-C formation. In contrast to the raw asphaltene precursor in this work, Vilaplana-Ortego *et al.* used a petroleum pitch as the precursor. Their precursor pitch had a higher carbon and lower sulfur content than the asphaltene in this work, which could lead to a different oxidative stabilization mechanism. Unfortunately, the elemental composition for the treated fibers was not discussed. Therefore, a comparison of the two materials in terms of composition changes is not possible.

The OF_{KNO3} samples showed a comparable increase in the oxygen content relative to fibers stabilized with H_2SO_4 or HNO_3; however, the C/H ratio remains low. Please note that the very large residual mass of sample OF_{KNO3} obtained after the CHNS measurement can also stem from residual K and not only oxygen on the fiber. This is indicated by white residue on the fiber surface (supporting information Fig. S1). It was further noted that the nitrogen content of the OF_{KNO3} samples were higher compared to fibers stabilized with H_2SO_4 or HNO_3. In fact, the nitrogen content of OF_{KNO3} (4.2 wt%) was more than double that of OF_{HNO3} (1.9 wt%). These observations indicated that there was meaningful retention of nitrates by the carbon fibers when treated with the potassium nitrate solution.

This reinforces the assertion that the presence of oxygen and nitrogen in the fiber does not on its own lead to successful structure stabilization. The way in which these elements are introduced determined whether the fiber was stabilized or not. For example, cross-linking reactions, either C-C formation or polycondensation reactions of oxygen functions, which can be promoted by acids, need to occur. This is further strengthened by other studies dealing with the formation of C-O-C groups during the oxidative stabilization of mesophase pitch-based fibers [13–15].

Another process that may occur is the elimination of volatile hydrogen-rich hydrocarbons, such as CH_4. Thermally induced hydrogen transfer reactions are pronounced in asphaltenes over the temperature range studied [25], but not the elimination of volatile hydrocarbons. The elimination of lighter material required treatment with oxidizing acids and not temperature alone. There are several examples of reactions between alkyl aromatics and HNO_3 that lead to elimination of water and alkyl fragments (as volatile hydrocarbons) [21], which could explain the observed increase in C/H ratio.

There was an increase in nitrogen content of OF_{HNO3} and OF_{H2SO4}, which is reflected by the decrease in the C/N ratio. While HNO_3 treatment could lead to incorporation of N, thereby lowering the C/N ratio, H_2SO_4 cannot induce any N incorporation. Therefore, the decrease in the C/N ratio must be connected to the removal of volatile hydrocarbons to cause both a decrease in C/N and an increase in C/H.

To investigate the hypothesis that HNO_3 acts in two ways, as an acid catalyst and as an oxidizing agent, green fibers were treated with a saturated solution of KNO_3 in HCl. Due to the lower solubility of KNO_3 in HCl, the same molar concentration as attained for HNO_3 could not be reached. With the acidification of KNO_3, the reacting system became a mixture of HCl-KCl-HNO_3-KNO_3. Indeed, the fibers maintain their fibrous structure after oxidation. This provided empirical support that it was not the nitrate that reacted, but the nitric acid formed by acidification.

However, as observed with potassium nitrate on its own, a significant amount of the salt remained on the fibers. This can be easily seen from the coverage of K that remains on the fibers (Supporting information, Figure S2). Residual K leads to defects in the carbon fiber structure after carbonization at temperatures above 800 °C.

3.3. Reaction progression with temperature

To monitor the reaction progression of the oxidation process with increasing temperature, the mass change during the stabilization process was recorded *via* TGA measurements under air for fibers that were treated in nitric acid at room temperature (Fig. 2a). A mass loss of 18 wt.% takes place from 230°C to 300°C.

Using the TGA results, the composition change of the fibers is examined at three different stages of the process – before any heat treatment (OF_{HNO3}-RT), at 140°C (OF_{HNO3}-140) as an intermediate temperature and at 230°C which is the beginning of the mass loss (OF_{HNO3}–230) (Table 1). Infrared spectra (IR) were also recorded during the heat treatment to display the changes in functional groups (Fig. 2b).

Up to 230°C the C/H ratio stays relatively constant, changing from 0.86 to 0.99, while the C/N and C/O ratios decrease noticeably, from 45.7 to 29.4 and from 20.4 to 8.9, respectively. This points to the incorporation of N and O into the fiber structure, potentially with some associated loss of hydrogen, likely as water.

This explanation is further supported by the IR spectra. The spectrum for raw asphaltene shows the symmetrical valence vibration υ_S (2955 cm^{-1}), and the asymmetrical valence vibration υ_{As} (2867 cm^{-1}), and the deformation vibration of both CH_2 and CH_3 in the region of 1450 cm^{-1} and 1370 cm^{-1}, respectively, as well as the C=C vibration at 1590 cm^{-1}. Peaks between 900 cm^{-1} and 700 cm^{-1} can be attributed to aromatic C-H bending. The IR spectrum of sample OF_{HNO3}-RT, which is the fiber immediately after acid treatment without applying any drying, washing or heating, can be found in Figure S5 in the supporting information. The spectrum shows the typical vibrations of nitric acid, which is attached to the fiber. Below 230°C, two vibrations at 1525 cm^{-1} and 1553 cm^{-1} occur, which are assigned to the υ_{As} vibration of NO_2 groups bonded to an aromatic or an aliphatic system. The signal at 1030

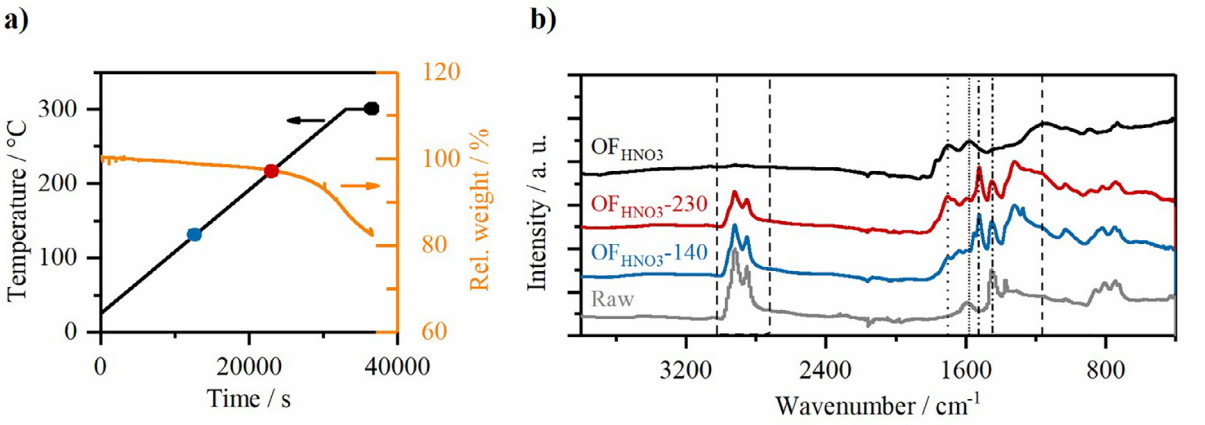

Fig. 2. a) Thermogravimetric analysis (TGA) conducted in synthetic air of sample OF_{HNO3}-RT. b) Infrared spectra of raw asphaltene (grey), OF_{HNO3}–140 (blue), OF_{HNO3}–230 (red) and OF_{HNO3} (black). Vertical lines correspond to some vibrations discussed in the text. Their changes are relevant to follow the mechanism explanation. (For interpretation of the references to color in this figure legend, the reader is referred to the web version of this article.).

cm^{-1} was tentatively assigned to S=O, but could also be due to C-O in several chemical environments. Additionally, the asymmetric, as well as the symmetric valence vibrations of aliphatic CH_2 and CH_3 groups and their deformation vibrations are still present. The relative reduction of these vibrations, as well as the disappearance of NO_2-related vibrations, occurs from 230°C to 300°C. Simultaneously, the deformation vibration of C=O in aryl-alkyl ketones (1704 cm^{-1}) and the broad υ_S vibration of C-O-C (1120 cm^{-1}) emerge. Furthermore, the C=C vibration (1590 cm^{-1}), which is attenuated between 140°C and 230°C, becomes stronger again, pointing to the formation of new C=C groups. These observations are supported by the CHNS analysis showing a decrease in the C/O ratio from 8.9 to 4.8, but an increase in the C/N ratio from 29.4 to 40.4 as the temperature was increased from 230°C to 300°C.

Based on these findings, the following sequence of reactions is proposed. First, NO_2-groups from nitric acid is incorporated into the fiber structure. This incorporation was viewed positively, following on a report that the char yield increased in relation to the extent of nitro-group incorporation for some polymers [26].

Mass loss below 230°C is gradual and limited. Above 230°C the rate of mass loss increases due to the decomposition of NO_2-groups, which disappeared from the infrared spectrum (Fig. 2b). This is consistent with the low bond dissociation energy of C-NO_2 bonds that are of the order 250 kJ/mol for nitromethane [27], and likely lower if decomposition produces a more stable carbon radical. This was also reflected in the reported Arrhenius activation energies for decomposition that were summarized by Zeman [28] having values mostly in the range 150–205 kJ mol^{-1} for various nitroalkanes and 115–195 kJ mol^{-1} for various nitroaromatics. In both instances values outside of these ranges were reported for some compounds. Indirect evidence of the reactions taking place is provided by the decreased in absorption by CH_3 and CH_2 groups and the increase in the absorption of C-O-C, C=C and C=O groups (Fig. 2b). Since the thermal decomposition is performed in an air atmosphere, the reactions following on thermal decomposition likely involves oxidation and other free radical reactions, such as hydrogen transfer and free radical addition.

The IR spectra of OF_{None}-300 supports the hypothesis that both the formation of C-O-C and the partial consumption of CH_3 and CH_2 groups are crucial for fiber structure retention for asphaltene-based carbon fibers. This stabilization process is not a pure surface phenomenon. SEM images and EDX analysis regarding the oxygen distribution inside the fibers indicate that this process is occurring over the whole fiber cross-section (Supporting Information, Figure S3).

3.4. Influence of acid concentration

To investigate the influence of acid concentration, green fibers were treated with four different HNO_3 acid concentrations varying from 10 vol.% to 40 vol.% (OF_{HNO3}–10%, OF_{HNO3}–20%, OF_{HNO3}–30% and OF_{HNO3}–40%). As reported by Vilaplana-Ortego *et al.,* a high acid concentration of more than 40 vol.% can result in the decomposition of the fibers and partial dissolution during the dipping process. This observation is consistent with the behavior of asphaltene-based fibers in this study. A concentration lower than 10 vol.% can lead to inhomogeneous fiber oxidation and partial melting of the fibers during the oxidative heat treatment. Therefore, the minimum HNO_3 concentration was chosen to be 10 vol.% and the maximum as 40 vol.% (based on a 15.8 N HNO_3 solution).

Oxidized fibers resulting from treatments using various acid concentrations were examined *via* SEM. Oxidized fibers obtained from the treatment with the lowest acid concentration (OF_{HNO3}–10%) had structural defects on the surface, as seen in Fig. 3a. In contrast, oxidized fibers obtained from the highest HNO_3 concentration treatment of 40 vol.% show homogenous and smooth surface with less defects (Fig. 3c). The difference in the surface smoothness becomes more pronounced after carbonization at 1500°C (Fig. 3b and d). SEM images of OF_{HNO3}–20% and OF_{HNO3}–30% follow the same trend and are shown in the Supporting Information (Figure S4).

The elemental compositions for the various acid treated samples differ somewhat (Table 2), but the C/H values are all in the range of 1.79 to 1.96. The nitrogen content of OF_{HNO3}–20% was lower than the other samples and the reason for this is not clear. The ratio of carbon to all heteroatoms was nevertheless an almost constant C/(NOS) ratio for the 4 different acid concentrations. The highest molar C/H ratio and lowest C/(NOS) ratio was found at the highest acid concentration (Fig. 4a).

After the carbonization process at 1500°C, the average diameters of the carbonized fibers had slight variations (Fig. 4b). The smallest fibers (8.8 µm) were obtained with the highest concentration of HNO_3 (40 vol.%), whereas the largest mean diameter (11.3 µm) was obtained with 10 vol.% of HNO_3. The difference between the 20 vol.% and 30 vol.% concentrations were less pronounced; however, with average diameters of 9.9 and 9.8 µm, respectively. Since the diameter differences were not very significant, the experiment was repeated with a second asphaltene fiber batch with a larger green fiber diameter. The same trend was observed (see Supporting Information, Figure S6). A third fiber batch with another asphaltene fiber diameter was processed as well. These

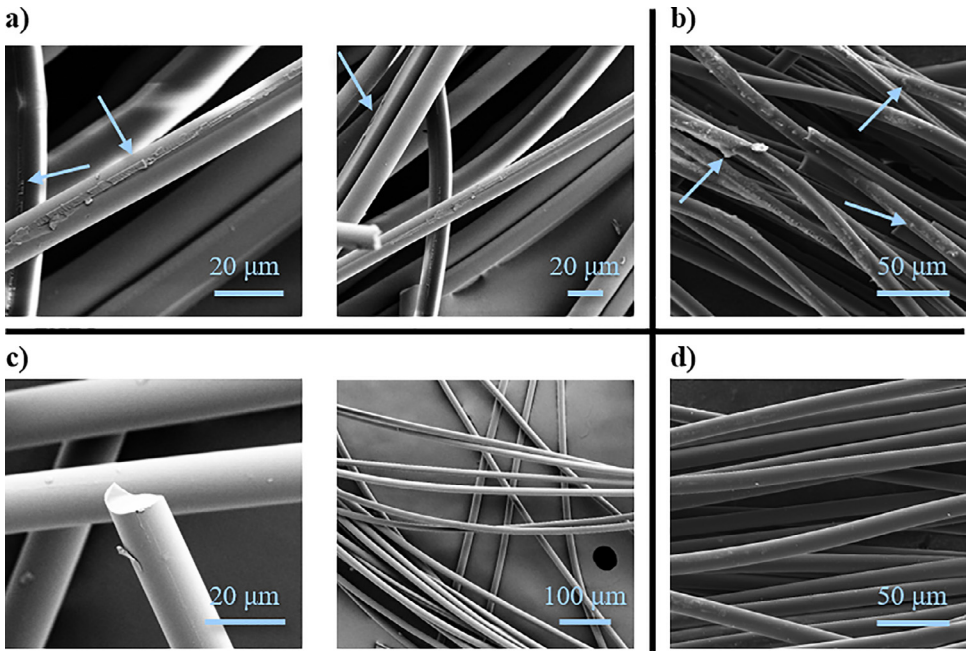

Fig. 3. SE micrographs of a) oxidized fibers and b) carbon fibers obtained with concentration of 10 vol.% HNO_3 treatment, and c) oxidized fibers and d) carbon fibers obtained with concentration 40 vol.% HNO_3 treatment.

Table 2
Elemental composition of different oxidized fibers synthesized using different HNO_3 concentration and fiber characteristics of the resulting carbon fibers. Composition is determined *via* elemental analysis.

CHNS analysis of oxidized fibers								Carbon fiber characteristics[d]		
Element content[a,b,c] / wt.%						Molar ratio		Dia-meter[e] / µm	Tensile strength[f] / MPa	Tensile Modulus[f] / GPa
Sample	C	H	N	S	O	C/H	C/NOS			
OF_{HNO3}–10%	64.94	3.03	3.36	5.80	22.87	1.79	2.97	11.3	418 (141)	18.2 (3.6)
OF_{HNO3}–20%	65.38	2.84	3.08	5.80	22.90	1.92	2.98	9.9	440 (199)	18.0 (4.5)
OF_{HNO3}–30%	65.10	2.90	3.39	5.93	22.68	1.87	2.94	9.8	630 (269)	27.9 (7.8)
OF_{HNO3}–40%	64.46	2.74	3.42	5.91	23.47	1.96	2.83	8.8	811 (371)	32.7 (14.1)

[a] Values are obtained as an average from 3 measurements (with a standard deviation smaller than 5%), or 2 measurements if the composition difference was smaller than 5%
[b] O content is calculated from the residual mass. Other components in the precursor material such as V and Ni are below 1500 ppm (determined *via* XRF, Supporting information Table S1). It is assumed that these element contents are constant for all fibers and therefore, changes in residual mass content are only due to changes in O content.
[c] From oxidized fibers.
[d] From corresponding carbonized fibers.
[e] Diameter determined as the average diameter from 60 or more single fibers.
[f] Average value from 20 single fiber measurements; standard deviation given in the brackets.

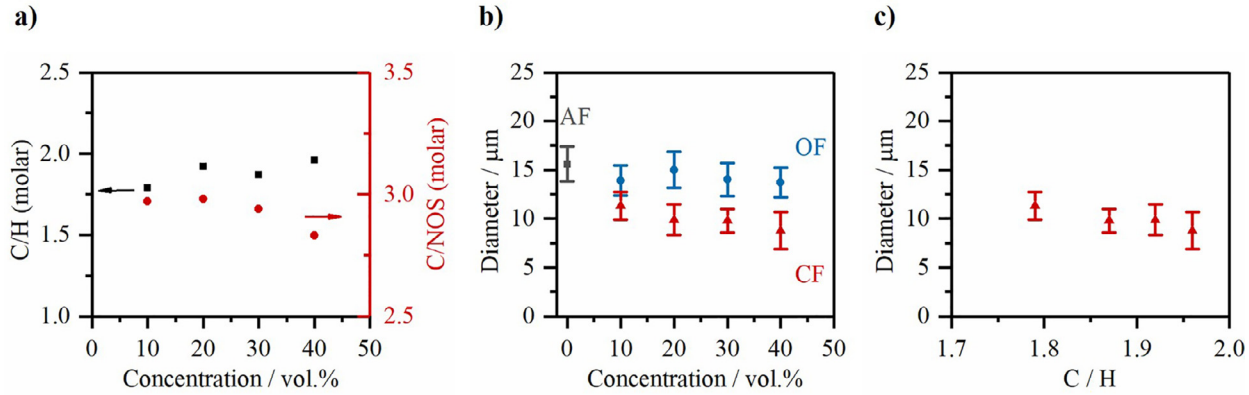

Fig. 4. a) Plots of C/H (black square) and C/NOS (red circle) molar ratios as a function of HNO_3 concentration. b) Fiber diameter versus HNO_3 concentration for asphaltene fibers (grey square), oxidized fiber (blue circle) and carbon fiber (red triangle). c) Carbon fiber diameter versus C/H ratio for OF_{HNO3}–10%, OF_{HNO3}–20%, OF_{HNO3}–30% and OF_{HNO3}–40%. (For interpretation of the references to color in this figure legend, the reader is referred to the web version of this article.).

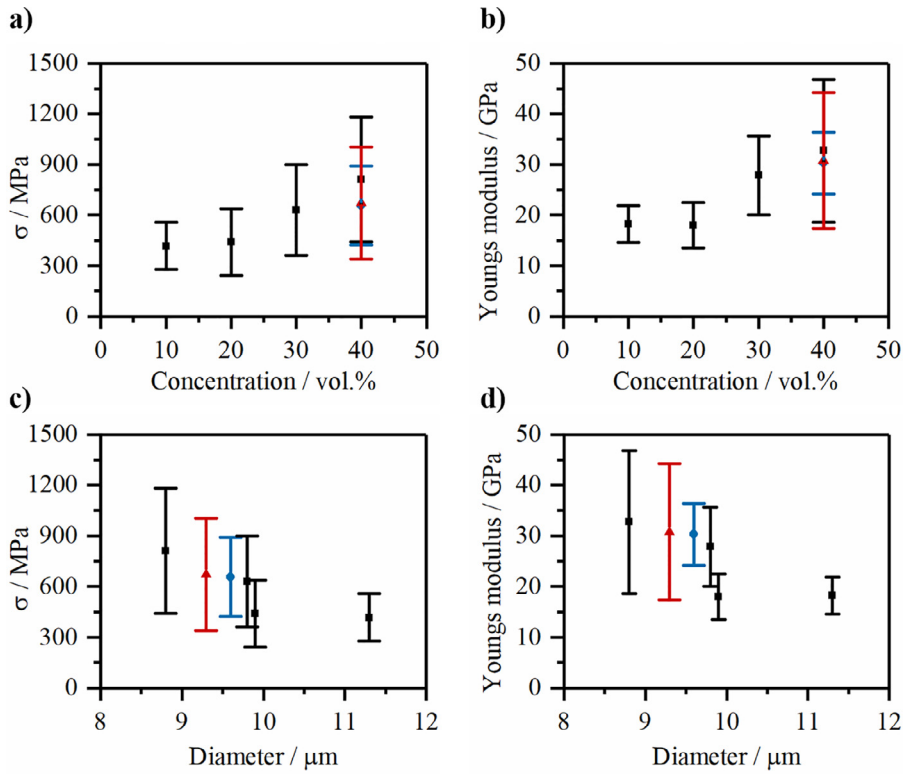

Fig. 5. a) Tensile strength and b) Young's modulus plotted as a function of HNO_3 concentration (batch 1). c) Tensile strength and d) Young's modulus plotted as a function of average carbon fiber diameter for batch 1 (black square) - OF_{HNO3}–10%, OF_{HNO3}–20%, OF_{HNO3}–30% and OF_{HNO3}–40%, batch 2 (red triangle) and batch 3 (blue circle). (For interpretation of the references to color in this figure legend, the reader is referred to the web version of this article.).

results will be discussed in a later section; however, there was a comparable diameter-concentration trend.

The yield after carbonization for all four acid concentrations samples were similar with values ranging from 37 wt.% - 38 wt.%. Hence, it is unlikely that the smaller fiber diameter with increasing acid concentration is caused by more pronounced CO_2 formation, which would cause higher carbon consumption. A possible explanation for the surface inhomogeneity and larger fiber diameter for fibers treated with lower acid concentration could be attributed to a lower fiber density. A higher C/H ratio indicates more oxidation reaction. This could result in a higher aromatic carbon content in the oxidized fibers. Thus, aromatic intramolecular interactions could be preferred, leading to a higher carbon fiber density and a slightly smaller average diameter. To test this hypothesis, the densities of CF-20% and CF-40% were determined as 1.56 and 1.57 g cm^3, respectively, *via* pycnometer methods using CCl_4 as a solvent. Because of possible solvent evaporation, low wettability and possible weighing errors, the obtained density difference cannot be regarded as significant. Assuming that a lower density is also related to a higher porosity in the carbon fiber, the micropore and mesopore volumes of CF-20% and CF-40% were determined *via* nitrogen physisorption. CF-40% has a pore volume of 0.03 cm^3 g^{-1}, whereas CF-20% exhibits a pore volume of 0.08 cm^3 g^{-1}. It should be noted that such a difference in pore volume (0.05 cm^3 g^{-1}) is not very significant either; however, considering the relative change in the C/H ratio and the carbon fiber diameter, the relative pore volume difference is not expected to be pronounced. Powder X-ray diffraction (P-XRD) did not indicate any difference in the d-spacings for the two carbon fibers (Supporting Information, Figure S7). Further testing with other asphaltene precursors and different diameter ranges should be done for confirmation.

The influence of acid concentration on the tensile performance of carbon fibers obtained from OF_{HNO3}–10%, OF_{HNO3}–20%, OF_{HNO3}–30%, and OF_{HNO3}–40% (Fig. 5a and b) was also investigated. In the current section, the samples are denoted as CF-10%, CF-20%, CF-30% and CF-40% according to the used acid concentration. With increasing acid concentration higher tensile strengths were achieved. Note that the large error bars stem from the broad diameter distribution of the carbon fibers (see Supporting Information, Figure S8). This was also the case for the Young's modulus. CF-40% has the highest average tensile strength and modulus with values of 811 MPa and 32.7 GPa, respectively. Individual fibers were able to reach even higher tensile strengths and moduli with values up to 1230 MPa and 47.2 GPa, respectively. This fiber performance can compete with other reported low-cost isotropic pitch-based carbon fibers [29,30]. However, the performance cannot match the high values for mesophase pitch-based carbon fibers or PAN-based carbon fibers [31–34]. The significantly lower cost of the unmodified asphaltene precursor still makes it a promising material for further research. It is noteworthy that the asphaltene precursor has been used without any further material improvement and it is a by-product from an industrial process. Furthermore, the carbonization temperature is only 1500°C. It has been reported that higher carbonization temperatures of 2500°C or even higher can significantly improve the tensile properties of carbon fibers, especially the Young's modulus, due to graphitization [35, 36].

To see whether the better tensile performance is due to the higher acid concentration or the smaller average carbon fiber diameter, two other fiber batches derived from the same raw asphaltene precursor were tested. The green fiber diameters of those two batches, designated as batch 2 and batch 3, were both larger than the green fibers for CF-40% (batch 1), with average green fiber diameters of 16.8 μm for batch 2 and 16.5 μm for batch 3. Both batches were treated in the same manner as CF-40%. The resulting average carbon fiber diameters were 9.6 μm and 9.3 μm, which are larger than the average diameter for sample CF-40% and com-

parable to CF-30% from batch 1. The effect on tensile properties is shown in Fig. 5c) and 5d). Better tensile performance can be attributed to smaller carbon fiber diameters and not to acid concentration. This behavior has also been reported by Tagawa *et al.* for PAN-, and mesophase pitch-based carbon fibers and is related to the non-isotropic statistical defect distribution in the fibers [37].

4. Conclusions

Carbon fibers have been prepared using a raw asphaltene precursor and a melt spinning process. Since the precursor materials displays a low softening point material, an acid treatment was applied to enable further heat treatment for the generation of carbon fibers. This work examined the mechanism for fiber structure stabilization. It was found that treatment with an oxidizing acid (HNO_3 or H_2SO_4) was required for retaining the fibrous structure during further processing and that the same could not be accomplished by non-oxidizing acid treatment (HCl). The increase in C/H ratio during thermal treatment after stabilization using HNO_3 was related to the thermal decomposition of nitro-groups that facilitated air oxidation and other thermal decomposition reactions leading to the loss of volatile hydrogen-rich products, such as light hydrocarbons.

Carbon fiber diameter was dependent on acid concentration, with a higher acid concentration leading to more pronounced fiber shrinkage and, therefore, smaller carbon fiber diameters. Smaller diameter fibers, which were obtained with higher acid concentrations, show better performance than larger diameter fibers with tensile strength and Young's modulus reaching 811 MPa and 32.7 GPa, respectively. The combination of a low cost precursor and a relatively low carbonization temperature (1500°C) makes asphaltene a promising candidate for the fabrication of carbon fibers for structural applications.

CRediT author statement

Desirée Leistenschneider: Conceptualization, Investigation, Writing - Original Draft, Visualization; **Peiyuan Zuo:** Investigation, Writing – Review; **Zahra Abedi:** Investigation, Writing – Review; **Yuna Kim:** Investigation, Writing – Review; **Douglas G. Ivey**: Writing - Review & Editing, Funding acquisition; **Arno de Klerk**: Writing - Review & Editing, Funding acquisition; **Xuehua Zhang**: Writing - Review & Editing, Funding acquisition, Project administration; **Weixing Chen:** Resources, Writing - Review & Editing, Supervision, Funding acquisition, Project administration

Declaration of Competing Interest

The authors declare no competing interest.

Acknowledgements

The authors would like to thank Alberta Innovates (Canada) for the financial support through the Bitumen Beyond Combustion program and the Natural Sciences and Engineering Research Council (NSERC) of Canada. The authors also thank Dr. Murray R. Gray, Dr. Paolo Bomben, and Dr. Axel Meisen for valuable discussions.

Supplementary materials

Supplementary material associated with this article can be found, in the online version, at doi:10.1016/j.cartre.2021.100090.

References

[1] V. Mechtcherine, A. Michel, M. Liebscher, K. Schneider, C. Großmann, Mineral-impregnated carbon fiber composites as novel reinforcement for concrete construction: Material and automation perspectives, Autom. Constr. 110 (2020) 103002, doi:10.1016/j.autcon.2019.103002.
[2] F.J. García-Mateos, R. Ruiz-Rosas, J. María Rosas, E. Morallón, D. Cazorla-Amorós, J. Rodríguez-Mirasol, et al., Activation of electrospun lignin-based carbon fibers and their performance as self-standing supercapacitor electrodes, Sep. Purif. Technol. 241 (2020) 116724, doi:10.1016/j.seppur.2020.116724.
[3] N. Vatin, S. Sultanov, A. Krupina, Comparison of thermal insulation characteristics of PIR, mineral wool, carbon fiber, in: V.Murgul aerogel, M. Pasetti, international scientific conference energy management of municipal facilities and sustainable energy technologies EMMFT 2018. EMMFT-2018 2018. Advances in intelligent systems and computing, Springer Cham. (2019) 877–883, doi:10.1007/978-3-030-19868-8_86.
[4] Y. Liu, S. Kumar, Recent progress in fabrication, structure, and properties of carbon fibers, Polym. Rev. 52 (2012) 234–258, doi:10.1080/15583724.2012.705410.
[5] M. Minus, S. Kumar, The processing, properties, and structure of carbon fibers, JOM 57 (2005) 52–58, doi:10.1007/s11837-005-0217-8.
[6] B.J. Kim, Y. Eom, O. Kato, J. Miyawaki, B.C. Kim, I. Mochida, et al., Preparation of carbon fibers with excellent mechanical properties from isotropic pitches, Carbon 77 (2014) 747–755, doi:10.1016/j.carbon.2014.05.079.
[7] T. Matsumoto, Mesophase pitch and its carbon fibers, Pure Appl. Chem. 57 (1985) 1553–1562, doi:10.1351/pac198557111553.
[8] D.A. Baker, T.G. Rials, Recent advances in low-cost carbon fiber manufacture from lignin, J. Appl. Polym. Sci. 130 (2013) 713–728, doi:10.1002/app.39273.
[9] E. Frank, L.M. Steudle, D. Ingildeev, J.M. Spörl, M.R. Buchmeiser, Carbon fibers: Precursor systems, processing, structure, and properties, Angew. Chem., Int. Ed. 53 (2014) 5262–5298, doi:10.1002/anie.201306129.
[10] D.D. Edie, M.G. Dunham, Melt spinning pitch-based carbon fibers, Carbon 27 (1989) 647–655, doi:10.1016/0008-6223(89)90198-X.
[11] M.S. Kim, D.H. Lee, C.H. Kim, Y.J. Lee, J.Y. Hwang, C.M. Yang, et al., Shell-core structured carbon fibers via melt spinning of petroleum- and wood-processing waste blends, Carbon 85 (2015) 194–200, doi:10.1016/j.carbon.2014.12.100.
[12] T.L. Dhami, L.M. Manocha, O.P. Bahl, Oxidation behaviour of pitch based carbon fibers, Carbon 29 (1991) 51–60, doi:10.1016/0008-6223(91)90094-Y.
[13] T. Matsumoto, I. Mochida, A structural study on oxidative stabilization of mesophase pitch fibers derived from coaltar, Carbon 30 (1992) 1041–1046, doi:10.1016/0008-6223(92)90134-I.
[14] G. Yuan, X. Li, X. Xiong, Z. Dong, A. Westwood, B. Li, et al., A comprehensive study on the oxidative stabilization of mesophase pitch-based tape-shaped thick fibers with oxygen, Carbon 115 (2017) 59–76, doi:10.1016/j.carbon.2016.12.040.
[15] T. Senda, Y. Yamada, M. Morimoto, N. Nono, T. Sogabe, S. Kubo, et al., Analyses of oxidation process for isotropic pitch-based carbon fibers using model compounds, Carbon 142 (2019) 311–326, doi:10.1016/j.carbon.2018.10.026.
[16] T. Yonemoto, J. Murakawa, M. Wada, T. Tadaki, Effect of NO_2 addition on oxidative stabilization process of pitch-based carbon fiber, Carbon 34 (1996) 1163–1165, doi:10.1016/0008-6223(96)84005-x.
[17] E. Vilaplana-Ortego, J. Alcañiz-Monge, D. Cazorla-Amorós, A. Linares-Solano, Stabilisation of low softening point petroleum pitch fibres by HNO_3, Carbon 41 (2003) 1001–1007, doi:10.1016/S0008-6223(02)00428-1.
[18] M.M. Ramirez-Corredores, The Science and Technology of Unconventional Oils, Academic Press, London, 2017.
[19] B. Schuler, Y. Zhang, F. Liu, A.E. Pomerantz, A.B. Andrews, L. Gross, et al., Overview of asphaltene nanostructures and thermodynamic applications, Energy Fuels 34 (2020) 15082–15105, doi:10.1021/acs.energyfuels.0c00874.
[20] Y.A. Casas, J.A. Duran, F.F. Schoeggl, H.W. Yarranton, Settling of asphaltene aggregates in n-alkane diluted bitumen, Energy Fuels 33 (2019) 10687–10703, doi:10.1021/acs.energyfuels.9b02571.
[21] Y. Ogata, Oxidations with nitric acid or nitrogen oxides, in: W.S. Trahanovsky (Ed.), Oxidation in Organic Chemistry. Part C, Academic Press, New York, 1978, pp. 295–342, doi:10.1016/B978-0-12-697252-8.50009-1.
[22] O.H. Larson, Methods of formation of the nitro group in aliphatic and alicyclic systems, in: H. Feuer (Ed.), The Chemistry of the Nitro and Nitroso Groups. Part I, Interscience, New York, 1969, pp. 301–348.
[23] W.M. Weaver, Introduction of the nitro group into aromatic systems, in: H. Feuer (Ed.), The Chemistry of the Nitro and Nitroso Groups. Part II, Interscience, New York, 1969, pp. 1–48.
[24] J. Gerard Lavin, Chemical reactions in the stabilization of mesophase pitch-based carbon fiber, Carbon 30 (1992) 351–357, doi:10.1016/0008-6223(92)90030-Z.
[25] N. Naghizada, G.H.C. Prado, A. De Klerk, Uncatalyzed hydrogen transfer during 100–250°C conversion of asphaltenes, Energy Fuels 31 (2017) 6800–6811.
[26] G.J. Fleming, Thermal analysis of nitro-substituted epoxide polymers, J. Appl. Polymer Sci. 13 (1969) 2579–2592.
[27] M.J.S. Dewar, J.P. Ritchie, J. Alster, Thermolysis of molecules containing NO_2 groups, J. Org. Chem. 50 (1985) 1031–1036.
[28] S. Zeman, Kinetic compensation effect and thermolysis mechanisms of organic polynitroso and polynitro compounds, Thermochim. Acta 290 (1997) 199–217.
[29] S. Ko, J.E. Choi, C.W. Lee, Y.P. Jeon, Modified oxidative thermal treatment for the preparation of isotropic pitch towards cost-competitive carbon fiber, J. Ind. Eng. Chem. 54 (2017) 252–261, doi:10.1016/j.jiec.2017.05.039.
[30] J. Yang, K. Nakabayashi, J. Miyawaki, S.H. Yoon, Preparation of isotropic pitch-based carbon fiber using hyper coal through co-carbonation with ethylene

bottom oil, J. Ind. Eng. Chem. 34 (2016) 397–404, doi:10.1016/j.jiec.2015.11.026.
[31] B.J. Kim, Y. Eom, O. Kato, J. Miyawaki, B.C. Kim, I. Mochida, et al., Preparation of carbon fibers with excellent mechanical properties from isotropic pitches, Carbon 77 (2014) 747–755, doi:10.1016/j.carbon.2014.05.079.
[32] V. Bermudez, A.A. Ogale, Adverse effect of mesophase pitch draw-down ratio on carbon fiber strength, Carbon 168 (2020) 328–336, doi:10.1016/j.carbon.2020.06.062.
[33] H. Shimanoe, T. Mashio, K. Nakabayashi, T. Inoue, M. Hamaguchi, J. Miyawaki, et al., Manufacturing spinnable mesophase pitch using direct coal extracted fraction and its derived mesophase pitch based carbon fiber, Carbon 158 (2020) 922–929, doi:10.1016/j.carbon.2019.11.082.
[34] K. Naito, Y. Tanaka, J.M. Yang, Y. Kagawa, Tensile properties of ultrahigh strength PAN-based, ultrahigh modulus pitch-based and high ductility pitch-based carbon fibers, Carbon 46 (2008) 189–195, doi:10.1016/j.carbon.2007.11.001.
[35] S. Wang, Z.H. Chen, W.J. Ma, Q.S. Ma, Influence of heat treatment on physical-chemical properties of PAN-based carbon fiber, Ceram. Int. 32 (2006) 291–295, doi:10.1016/j.ceramint.2005.02.014.
[36] L. Fischer, W. Ruland, The influence of graphitization on the mechanical properties of carbon fibers, Colloid Polym. Sci. 258 (1980) 917–922, doi:10.1007/BF01584920.
[37] T. Tagawa, T. Miyata, Size effect on tensile strength of carbon fibers, Mater. Sci. Eng. 238 (1997) 336–342, doi:10.1016/S0921-5093(97)00454-1.